Emulation of Wind Dynamics Using a Programmable Three-phase Inverter

Rahul Mallik*, Kamakshi Tatkare*, Weiqian Cai, Brian Johnson
Chandra Family Department of Electrical and Computer Engineering, The University of Texas at Austin, TX 78712, USA
Email: {rmallik, kamakshi, stratoscwq, and b.johnson}@utexas.edu

***Abstract*—This paper presents a cost-effective and resource-efficient approach to emulate the dynamics of a direct-drive wind turbine using a three-phase inverter. The fast responsiveness offered by power electronics enables us to obtain a means of high-fidelity wind turbine emulation. To accurately capture the limits of valid emulation, a per-unitized model is introduced whose base power can be adjusted. Analysis of the small-signal normalized model reveals instability for turbine models that have lower base values and whose small mechanical time constants have insufficient timescale separation from the inverter controls. The proposed approach is validated on a 1 kW laboratory-scale prototype.**

***Index Terms*—hardware emulation, wind energy, small-signal stability, direct-drive machines**

I. Introduction

As the fraction of wind energy grows within modern grids, it is necessary to realize experimental setups that capture the behavior of wind systems in an accurate manner. However, this objective is hampered by the fact that real wind turbine systems are impractically large for laboratory-scale experiments. Accordingly, most observations are limited to simulations and large-scale field experiments. This work aims to bridge this gap by offering a convenient means of replicating wind system dynamics in a purely electronic setting with reasonably sized hardware that can fit on a bench. The lack of mechanical hardware breaks down logistical barriers and reduces hazards. Our approach encompasses the full chain of subsystems where we start from the wind velocity itself and end at the machine stator terminals. The various models are woven together, discretized, and programmed on a modestly sized converter. After characterizing the stability of our approach and establishing fundamental scaling limits, experimental results are shown on a 1 kW three-phase inverter.

The idea of wind-turbine emulation is old news and prior methods generally rely on electromechnical setups with back-to-back machines [1], [2], [3], [4], [5]. In such a setting, one machine mimics the turbine and the other acts as a generator that feeds downstream electronics. Such approaches suffer from two main drawbacks. First, the use of multiple machines drives up costs, complexity, and resource requirements. Secondly, the smaller machines in such systems necessitate a torque compensation loop [6], [7] to match the inertia of realistic generators that are significantly larger in size. These compensation loops may also introduce instabilities [8]. Our approach bypasses these issues by eliminating all rotating machinery and moving squarely to the domain of electronics.

Power-electronics-based emulation has been studied in the context of compressors [9] and electric vehicles [10]. In such works, a current controller is typically used whose reference is derived from a virtual stator current that comes from a digitized machine model. However, this method can be problematic at lower switching frequencies where current control loops are slower and machine dynamics may encroach on the timescales of the current loop. To mitigate this problem, the paper in [11] presents a method where impedance is regulated such that the inverter plant may be approximated as matching the emulated machine plant. Our method circumvents these challenges by the use of sufficiently high switching frequencies with SiC devices which in turn enables fast current control.

The main contribution of this paper is twofold. First we establish a detailed dynamic model for a direct drive wind turbine that incorporates the inverter control for emulation. Secondly, we derive fundamental limits that guarantee stable closed-loop emulation. The rest of this paper is structured as follows. In section II, we formulate the analytical dynamics of the wind turbine system in which the wind, turbine, and synchronous generator physical models are included. An emulation controller relying on such model is then proposed for implementation on three-phase inverters. In Section III, the stability of such a controller is assessed with varying system power scalings. Finally, the emulation controller is validated on hardware in Section IV.

II. System Modeling

A. Electromechanical System

For this paper we consider a direct-drive wind turbine whose model encompasses the blades, hub, and synchronous generator. The system of interest is illustrated in Fig. 1 [12]. Notationwise, the subscripts b, h, and g stand for blade, hub, and generator, respectively. Additionally, J_x, d_x, and ω_x are the inertia, self-damping, and rotational speed, $\forall\, x \in \{\mathrm{b}, \mathrm{h}, \mathrm{g}\}$, respectively. Furthermore, d_{xy}, k_{xy}, and T_{xy} are the damping, stiffness, and the torque on the shaft, respectively, between x and y where, $x, y \in \{\mathrm{b}, \mathrm{h}, \mathrm{g}\}$. Rotational dynamics are then

This work was supported by the National Science Foundation CAREER Award under grant number 2314415.

* Rahul Mallik and Kamakshi Tatkare are co-first authors. Corresponding author is Rahul Mallik.

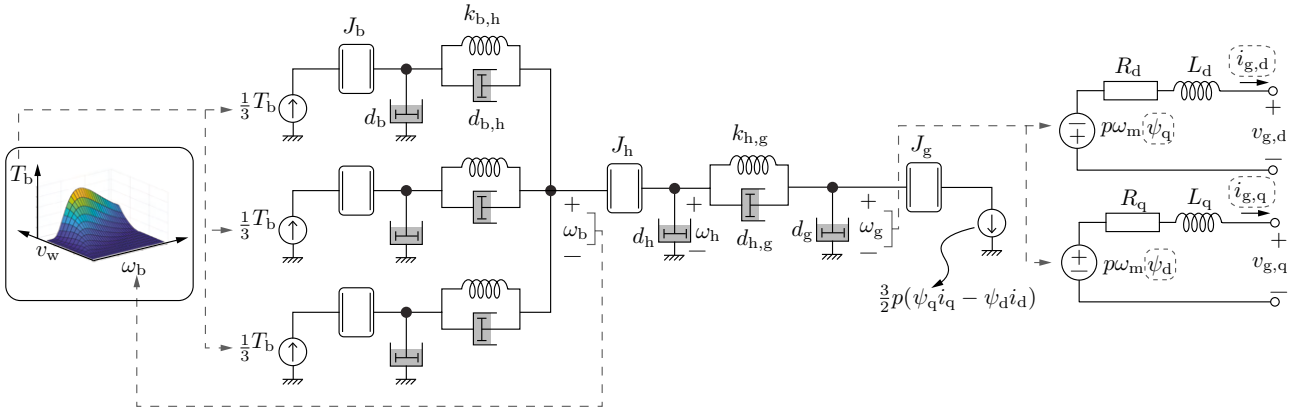

Figure 1: System model which consists of a three-blade wind turbine, hub, and generator is shown with appropriate coupling between the mechanical and electromechanical systems.

given by

$$\frac{J_\mathrm{b}}{d_\mathrm{b}}\frac{d\omega_{\mathrm{b},i}}{dt} = -\omega_{\mathrm{b},i} + \frac{1}{d_\mathrm{b}}\left(\frac{1}{3}T_\mathrm{b} - T_{\mathrm{bh},i}\right) \quad \forall i \in \{1,2,3\}, \tag{1a}$$

$$\frac{J_\mathrm{h}}{d_\mathrm{h}}\frac{d\omega_\mathrm{h}}{dt} = -\omega_\mathrm{h} + \frac{1}{d_\mathrm{h}}\left(\sum_{i=1}^{3} T_{\mathrm{bh},i} - T_\mathrm{hg}\right), \tag{1b}$$

$$\frac{J_\mathrm{g}}{d_\mathrm{g}}\frac{d\omega_\mathrm{g}}{dt} = -\omega_\mathrm{g} + \frac{1}{d_\mathrm{g}}\left(T_\mathrm{hg} - \underbrace{\frac{3}{2}p\left(\psi_\mathrm{q}i_{\mathrm{g,q}} - \psi_\mathrm{d}i_{\mathrm{g,d}}\right)}_{\text{electrical torque}}\right), \tag{1c}$$

where the index i denotes the i-th blade for a three-blade wind turbine and the d- and q-axis flux linkages are

$$\psi_\mathrm{q} = L_\mathrm{q}i_{\mathrm{g,q}}, \quad \psi_\mathrm{d} = L_\mathrm{d}i_{\mathrm{g,d}} + \phi_\mathrm{m}.$$

The dynamics of the angle between the blade and hub, $\theta_{\mathrm{bh},i}$, and the hub and generator, θ_hg, are expressed as

$$\frac{d_\mathrm{bh}}{k_\mathrm{bh}}\dot{\theta}_{\mathrm{bh},i} = -\theta_{\mathrm{bh},i} + \frac{1}{k_\mathrm{bh}}T_{\mathrm{bh},i} \tag{2a}$$

$$\frac{d_\mathrm{hg}}{k_\mathrm{hg}}\dot{\theta}_\mathrm{hg} = -\theta_\mathrm{hg} + \frac{1}{k_\mathrm{hg}}T_\mathrm{hg}, \tag{2b}$$

where $\theta_{\mathrm{bh},i} = \int(\omega_\mathrm{b} - \omega_\mathrm{h})dt$ and $\theta_\mathrm{hg} = \int(\omega_\mathrm{h} - \omega_\mathrm{g})dt$. Wind power may be expressed [13] as

$$P_\mathrm{w} = \frac{1}{2}\rho\pi R^2 v_\mathrm{w}^3 C_\mathrm{p}(\lambda,\beta), \tag{3}$$

where ρ is the air density, R is the radius of the circle swept by the wind turbine, and v_w is the upstream free wind velocity. The power coefficient, $C_\mathrm{p}(\lambda,\beta)$ is obtained as

$$C_\mathrm{p}(\lambda,\beta) = c_1\left(c_2\lambda_i - c_3\beta - c_4\right)e^{-c_5\lambda_i} + c_6\lambda$$

where the constants are $c_1 = 0.5176, c_2 = 116, c_3 = 0.4, c_4 = 5, c_5 = 21$, and $c_6 = 0.0068$, and β is the pitch angle in degrees. The tip speed ratio, λ, and the variable λ_i are given by

$$\lambda = \frac{R\omega_\mathrm{b}}{v_\mathrm{w}}, \qquad \lambda_i = \frac{1}{\lambda + 0.08\beta} - \frac{0.035}{\beta^3 + 1}.$$

The PMSG dynamics is given by

$$L_\mathrm{d}\frac{d}{dt}i_{\mathrm{g,d}} = -R_\mathrm{g}i_{\mathrm{g,d}} + p\omega_\mathrm{g}\psi_\mathrm{q} - v_{\mathrm{g,d}} \tag{4}$$

$$L_\mathrm{q}\frac{d}{dt}i_{\mathrm{g,q}} = -R_\mathrm{g}i_{\mathrm{g,q}} - p\omega_\mathrm{g}\psi_\mathrm{d} - v_{\mathrm{g,q}} \tag{5}$$

where p is the number of pole pairs, R_g is the coil resistance, ψ_d and ψ_q are the flux linkages on the d- and q-axis, respectively. L_d and L_q represent the d- and q-axis inductance respectively. A three-phase electrical signal, $x_\mathrm{abc} := [x_\mathrm{a}, x_\mathrm{b}, x_\mathrm{c}]^\top$ and its corresponding signal in dq-frame, $x_\mathrm{dq} := [x_\mathrm{d}, x_\mathrm{q}]^\top$ are related as $x_\mathrm{abc} = \Gamma^\top(\theta_\mathrm{g})x_\mathrm{dq}$, where $\theta_\mathrm{g} = \int_0^t \omega_\mathrm{g}d\sigma$, and $\Gamma(\theta_\mathrm{g})$ is defined as:

$$\Gamma(\theta_\mathrm{g}) = \frac{2}{3}\begin{bmatrix} \cos\theta_\mathrm{g} & \cos\left(\theta_\mathrm{g} - \frac{2\pi}{3}\right) & \cos\left(\theta_\mathrm{g} - \frac{4\pi}{3}\right) \\ -\sin\theta_\mathrm{g} & -\sin\left(\theta_\mathrm{g} - \frac{2\pi}{3}\right) & -\sin\left(\theta_\mathrm{g} - \frac{4\pi}{3}\right) \end{bmatrix}.$$

B. Emulation Using a Three Phase Inverter

A three-phase inverter is used to mimic the behavior of a wind turbine. As shown in Fig. 2, a microcontroller implements the dynamical equations in (1a), (1b), (1c), (2a), and (2b) at an interval of 1 millisecond. The input to these dynamical equations is the wind power, while the output is the torque, T_hg, which is then fed to the mathematical model of PMSG given by (4)–(5). To establish an exact mapping between the wind turbine system and the three phase inverter with its inductive filter (shown in two gray boxes in Fig. 2), we do two things. First, the mathematical model of PMSG in (4)–(5) is solved, where we substitute $v_{\mathrm{g,dq}} = v_{\mathrm{o,dq}}$. Secondly, a current controller regulates the inverter current, i_dq, such that

$$i_\mathrm{dq}^\star = -i_{\mathrm{g,dq}} \Rightarrow i_\mathrm{d}^\star = -i_{\mathrm{g,d}}, \quad i_\mathrm{q}^\star = -i_{\mathrm{g,q}} \tag{6}$$

To that end, we use a proportional-integral (PI) controller with a proportional and integral gain, k_p and k_i, respectively. For a current control bandwidth of ω_bw, the controller gains are chosen as $k_\mathrm{p} = \omega_\mathrm{bw}L$ and $k_\mathrm{i} = \omega_\mathrm{bw}R$. Feedforward and decoupling controls are incorporated into the control system. To avoid overcurrents, the commands of the current controller are restricted by a saturation block and a related anti-windup mechanism, where we set $I_\mathrm{max} = 15A$. Using the integral

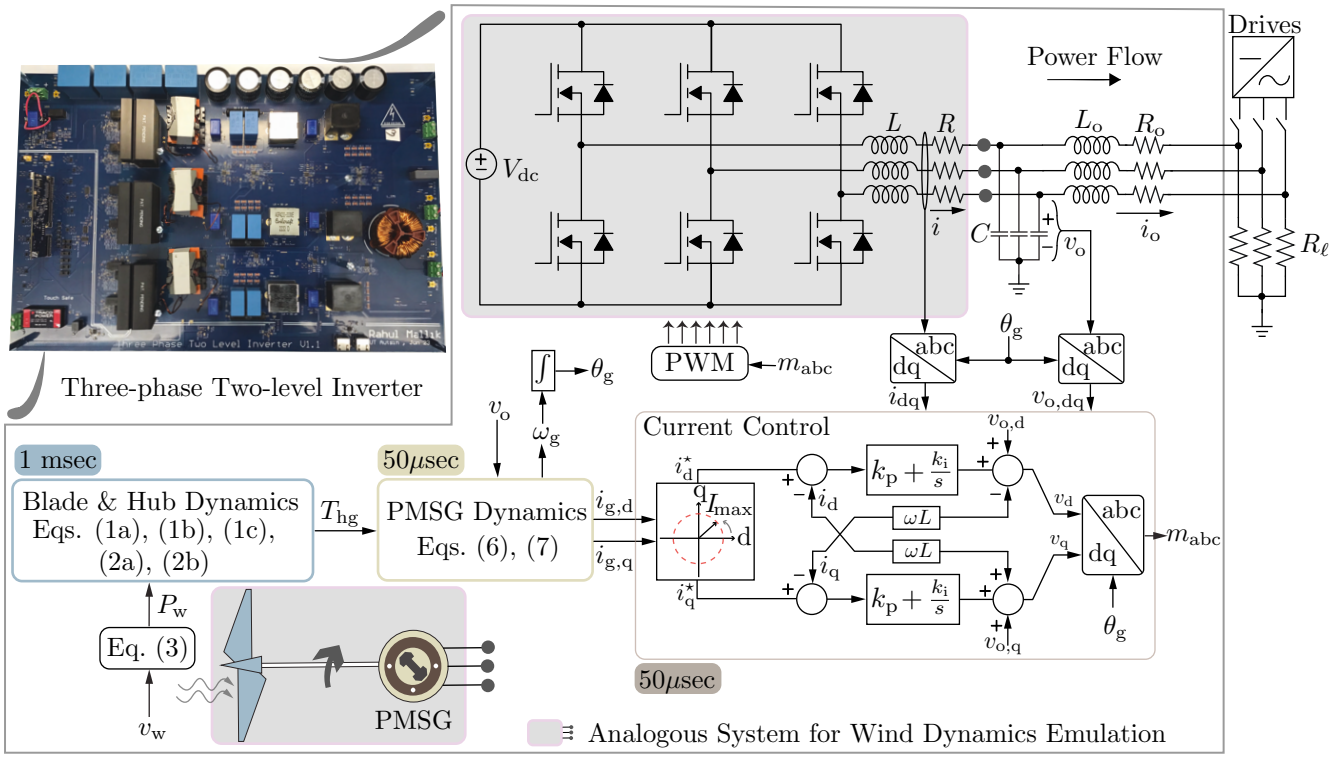

Figure 2: Power electronics emulation of the blade, hub, and permanent magnet synchronous generator on a digitally-controlled 1 kW three-phase two-level inverter.

states $\dot{\gamma}_{dq} := [\dot{\gamma}_d, \dot{\gamma}_q]^\top = [i^\star_{dq} - i_{dq}]$ the averaged switch terminal voltages are as follows:

$$\begin{aligned} v_d &= k_p \dot{\gamma}_d + k_i \gamma_d + v_{o,d} - \omega L i_q, \\ v_q &= k_p \dot{\gamma}_q + k_i \gamma_q + v_{o,q} + \omega L i_d \end{aligned} \tag{7}$$

Ignoring switching delays, the inverter is modulated to ensure that the three-phase switch terminal voltages are equal to $v_{abc} = \Gamma(\theta_g) v_{dq}$. The dynamics of inverter current, i_{dq}, capacitor voltage, $v_{o,dq}$, and output current, $i_{o,dq}$, is given by [14]

$$\begin{bmatrix} \dot{i}_d \\ \dot{i}_q \end{bmatrix} = \begin{bmatrix} -\frac{R}{L} & \omega \\ -\omega & -\frac{R}{L} \end{bmatrix} \begin{bmatrix} i_d \\ i_q \end{bmatrix} + \frac{1}{L} \begin{bmatrix} v_d - v_{o,d} \\ v_q - v_{o,q} \end{bmatrix}, \tag{8a}$$

$$\begin{bmatrix} \dot{i}_{o,d} \\ \dot{i}_{o,q} \end{bmatrix} = \begin{bmatrix} -\frac{R_o}{L_o} & \omega \\ -\omega & -\frac{R_o}{L_o} \end{bmatrix} \begin{bmatrix} i_{o,d} \\ i_{o,q} \end{bmatrix} + \frac{1}{L_o} \begin{bmatrix} v_{o,d} - e_d \\ v_{o,q} - e_q \end{bmatrix}, \tag{8b}$$

$$\begin{bmatrix} \dot{v}_{o,d} \\ \dot{v}_{o,q} \end{bmatrix} = \begin{bmatrix} 0 & \omega \\ -\omega & 0 \end{bmatrix} \begin{bmatrix} v_{o,d} \\ v_{o,q} \end{bmatrix} + \frac{1}{C} \begin{bmatrix} i_d - i_{o,d} \\ i_q - i_{o,q} \end{bmatrix}, \tag{8c}$$

where the terminal voltage, e_{dq} can be written as $e_{dq} = R_\ell i_{o,dq}$, when a three phase resistance, R_ℓ is connected at the output of the three-phase inverter. Under perfect tracking, when the inverter-side current, i_{dq}, matches the machine currents, $i_{g,dq}$, the machine terminal voltage, $v_{g,dq}$ becomes equal to the capacitor voltage, $v_{o,dq}$. Unlike the slower mechanical dynamics of the turbine, the electrical dynamics of the PMSG and the current controller is implemented once every 50μ sec.

III. Stability Analysis

A perfect emulation can be ensured as long as the fastest time-constant in the emulated system is sufficiently slower than the current controller bandwidth. In particular, for smaller power turbines, the mechanical time constants, J_x/d_x and d_{xy}/k_{xy} become comparable to $1/\omega_{bw}$. To capture this instability and obtain bounds on emulation, we now introduce a per-unitized model whose the base quantities for power, voltage, and frequency is defined as S_B, V_B, and ω_B, respectively. The base quantities of torque, T_B, and impedance, Z_B, are obtained from the following equality $S_B = T_B \omega_B = 3V_B^2/Z_B$. Both inertia ($J_x$) and damping ($d_x, d_{xy}$) have S_B/ω_B^2 as their base quantity, whereas the base for stiffness coefficient (k_{xy}) is T_B. Finally, the base for flux linkage, ϕ_m, is V_B/ω_B. Using these base quantities, we per-unitize the dynamical system discussed in Section II where details of the system inertia, damping, and stiffness constant are shown in Table I. Thereafter, a small-signal stability analysis of the normalized system for various base power is used to demonstrate the boundaries of stable emulation. We gather the dynamics of the nonlinear system into $\dot{x} = f(x, u)$ where $x \in \mathcal{R}^{15}$ is composed as

$$x = [\omega_b, \omega_h, \omega_g, \theta_{bh}, \theta_{hg}, i_{g,dq}, i_{dq}, \gamma_{dq}, v_{o,dq}, i_{o,dq}]$$

and $f(x, u)$ is the nonlinear flows delineated in Sec. II. The wind velocity, v_w, is the external input, u. We set $f(x, u) = 0$ to obtain the equilibrium solution x_{eq} and denote the Jacobian matrix $\mathcal{J} := \partial f(x, u)/\partial x$. To analyze the small-signal

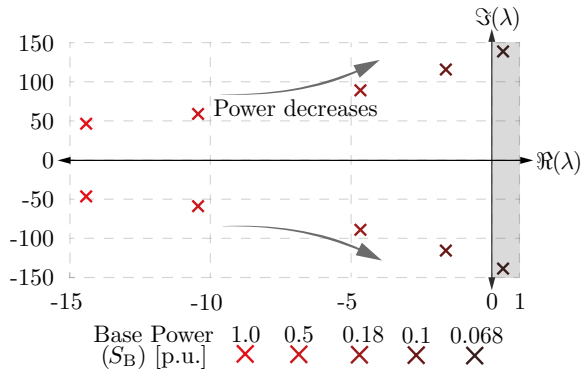

(a)

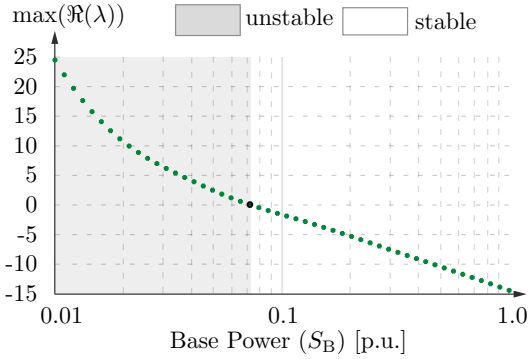

(b)

Figure 3: Eigenmap of per-unitized wind turbine emulation system shows dominant eignevalues approaching right half plane at lower base powers.

stability of the system for a given wind velocity, v_w, and a given system base power, S_B, we examine the corresponding eigenvalues of $\mathcal{J}(x_{eq}, v_w)$.

Fig. 3 (a) shows the eigenvalues as the system power is varied. As we attempt to replicate smaller power rated wind turbines, the related mechanical time constants increase and begin to interact with the inverter's current control loop. As shown in Fig. 3 (b), this interaction becomes unstable for a critical power of 0.072 pu when the largest eigenvalues become positive.

IV. Experimental Results

To validate the proposed emulation technique, the set-up shown in Fig. 2 implemented with a 1 kW three phase inverter. Ideally, this setup would connect to a test direct-drive inverter; however, for simplicity, we use a passive load to draw power from the emulated wind turbine system. In Fig. 4 we demonstrate that as the wind velocity is increased from 2 m/s to 14 m/s, the power flow is increased, which is reflected in the dc currents, i_{dc}, and the ac currents $i_{o,abc}$. With increasing power, due to the emulated dynamics, as expected, the PMSG voltage as well as its frequency increases, as shown by the zoomed waveforms in Fig. 4 (b). When the wind velocity is successively ramped down, the decrease in power is captured in Fig. 4 (a). We successfully demonstrate robustness of the emulation against a sudden load transient, we switch between two load resistance of 22 Ω and 9 Ω at the peak wind velocity in Fig. 4 (c). To demonstrate the instability that sets in for emulating lower power rated wind turbines, we vary the wind velocity from 6 to 14 m/s for three different base powers of 1 pu, 0.18 pu, and 0.1 pu. Corresponding results for each base power is shown in Fig. 5 (a), (b), and (c), respectively. At 1 pu power, the emulation is consistent regardless of the wind speed. However, for 0.18 pu power, instability begins to occur at very high wind velocities, while for 0.1 pu power, the emulation is unstable at all wind speeds. The mismatch between the theoretical (0.07 pu) and experimental (0.18 pu) critical power can be attributed to the linear approximation of the nonlinear system dynamics where eigenvalues close to the imaginary axis of the linearized system cannot conclusively predict a corresponding stable nonlinear system.

Table I: System Parameters

	Symbol	Description	Value	Units
Inverter	S_B	Base power	1	kW
	V_B	Base voltage	100	V
	ω_B	Base freq.	60	Hz
	ω_{sw}	Switching freq.	100	kHz
	L, L_o	Inductance	$122, 33$	μH
	R, R_o	Resistance	$0.4, 0.1$	Ω
	C	Capacitance	7	μF
	V_{dc}	Input dc voltage	300	V
	$\omega_{bw,i}$	Controller BW	2000	Hz
	R_ℓ	Load resistance	22	Ω
Wind Turbine	R	Blade radius	3	m
	ρ	Air density	1.204	kg/m^3
	β	Pitch angle	0	deg.
	J_b	Blade inertia	0.7394	kg-m^2
	J_h	Hub inertia	0.0132	kg-m^2
	J_g	PMSG inertia	0.1642	kg-m^2
	d_b, d_h, d_g	Self-damping	$[5, 12, 12] \times 10^{-3}$	kg-m^2/s
	d_{bh}, d_{hg}	Damping	$13.89, 11.57$	kg-m^2/s
	k_{bh}, k_{hg}	Stiffness	$349.9, 509.5$	kg-m^2/s^2
PMSG	p	Pole pairs	2	
	ω_g^{nom}	Nominal speed	542.99	rpm
	L_d, L_q	Inductance	$0.02, 0.04$	H
	R_g	Resistance	0.01	Ω
	ϕ_m	Peak flux	0.833	V/(rad/s)

V. Conclusion

We demonstrated a dynamic wind turbine emulation using a three-phase inverter for direct drive applications. We used a small-signal stability analysis of the per-unitized model to check the boundaries of feasible stable emulation. Specifically, we demonstrated that, at low per-unit power, the mechanical time constants interact with the current controller of the inverter, causing an unstable emulation. We verify our proposed approach on a 1 kW inverter.

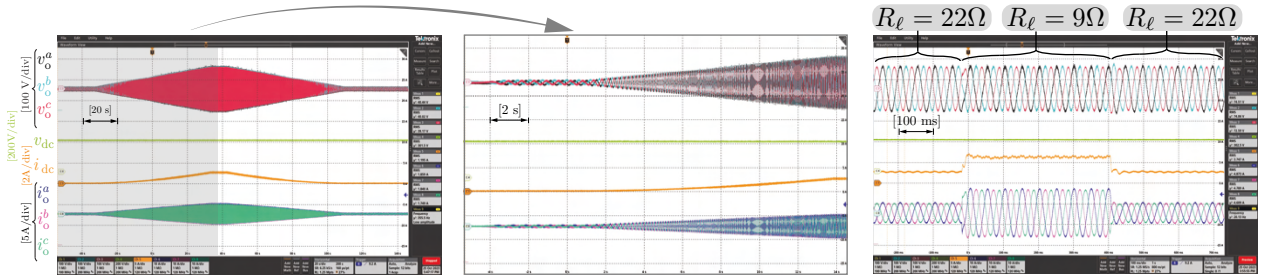

Figure 4: Experimental results demonstrate the wind emulation implementation for wind velocity ramp from 2 m/s to 14 m/s with a fixed load resistance in (a) and (b). In (c) we show a stable emulation during a load transient at the peak wind velocity.

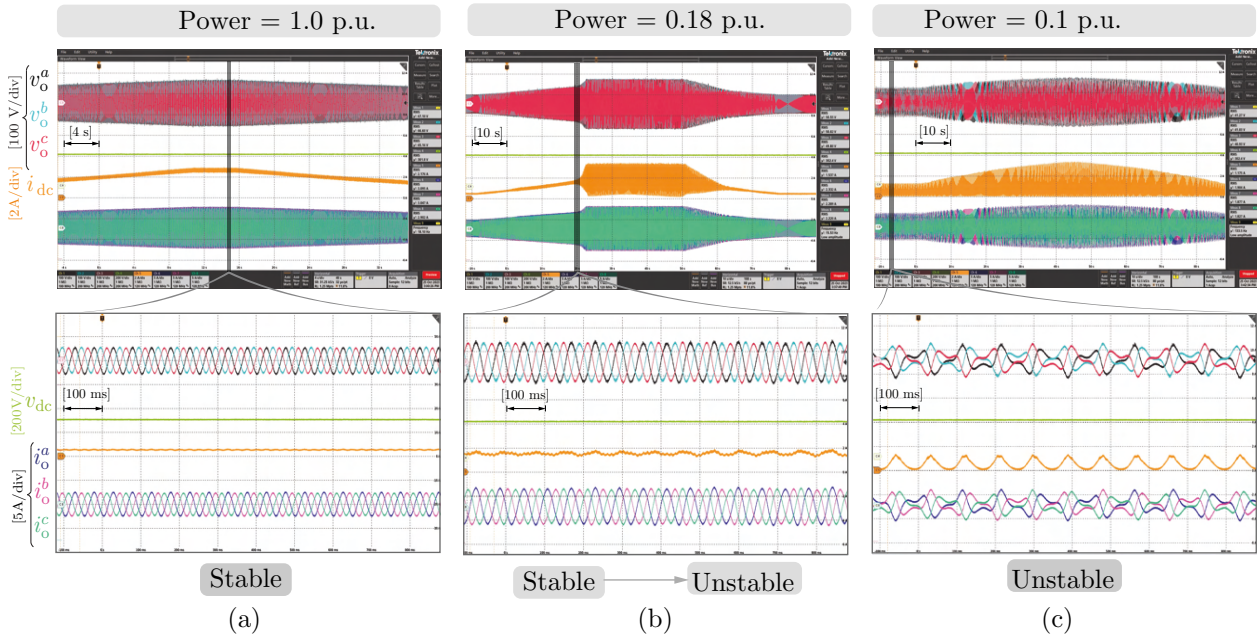

Figure 5: Instability in emulation is demonstrated for progressively decreasing base powers. Emulation is stable for 1 pu power in (a), unstable for 0.18 pu power at higher wind velocity in (b), and unstable for 0.1 pu power at all wind velocities in (c).

References

[1] A. Hazzab, H. Gouabi, M. Habbab, M. Rezkallah, H. Ibrahim, and A. Chandra, "Wind turbine emulator control improvement using non-linear pi controller for wind energy conversion system: Design and real-time implementation," *International Journal of Adaptive Control and Signal Processing*, vol. 37, no. 5, pp. 1151–1165, 2023.

[2] J. Castelló, J. M. Espí, and R. García-Gil, "Development details and performance assessment of a wind turbine emulator," *Renewable Energy*, vol. 86, pp. 848–857, 2016.

[3] I. Moussa, A. Bouallegue, and A. Khedher, "New wind turbine emulator based on dc machine: hardware implementation using fpga board for an open-loop operation," *IET Circuits, Devices & Systems*, vol. 13, no. 6, pp. 896–902, 2019.

[4] P.-Y. Chen, K.-W. Hu, Y.-G. Lin, and C.-M. Liaw, "Development of a prime mover emulator using a permanent-magnet synchronous motor drive," *Transactions on Power Electronics*, vol. 33, no. 7, pp. 6114–6125, 2018.

[5] J. R. de Oliveira and A. L. Andreoli, "Wind turbine emulator: A tool for experimental and computational study," *Latin America Transactions*, vol. 19, no. 11, pp. 1832–1839, 2021.

[6] S.-H. SOng, B.-C. Jeong, H.-I. Lee, J.-J. Kim, J.-H. Oh, and G. Venkataramanan, "Emulation of output characteristics of rotor blades using a hardware-in-loop wind turbine simulator," in *APEC*, vol. 3, 2005.

[7] H. Kojabadi, L. Chang, and T. Boutot, "Development of a novel wind turbine simulator for wind energy conversion systems using an inverter-controlled induction motor," *Transactions on Energy Conversion*, vol. 19, no. 3, pp. 547–552, 2004.

[8] R. Nair and G. Narayanan, "Emulation of wind turbine system using vector controlled induction motor drive," *Transactions on Industry Applications*, vol. 56, no. 4, pp. 4124–4133, 2020.

[9] K. Saito and H. Akagi, "A real-time real-power emulator of a medium-voltage high-speed induction motor loaded with a centrifugal compressor," *Transactions on Industry Applications*, vol. 55, no. 5, pp. 4821–4833, 2019.

[10] K. S. Amitkumar, R. S. Kaarthik, and P. Pillay, "A versatile power-hardware-in-the-loop-based emulator for rapid testing of transportation electric drives," *Transactions on Transportation Electrification*, vol. 4, no. 4, pp. 901–911, 2018.

[11] K. Ma and Y. Song, "Power-electronic-based electric machine emulator using direct impedance regulation," *Transactions on Power Electronics*, vol. 35, no. 10, pp. 10 673–10 680, 2020.

[12] O. Wasynczuk, D. T. Man, and J. P. Sullivan, "Dynamic behavior of a class of wind turbine generators during random wind fluctuations," *Power Engineering Review*, vol. PER-1, no. 6, pp. 47–48, 1981.

[13] E. Hau, *Wind Turbines - Fundamentals, Technologies, Application, Economics*. Springer Berlin, Heidelberg, 2013.

[14] M. Lu, R. Mallik, B. Johnson, and S. Dhople, "Dispatchable virtual-oscillator-controlled inverters with current-limiting and mppt capabilities," in *ECCE*, 2021, pp. 3316–3323.